

Structural and electric investigations of Al-doped nano nickel ferrite

Dr. Salam H. Ali Al-Hadad

Applied Sciences Department, University of Technology/ Baghdad.

Shahad Humam Sulaiman

Applied Sciences Department, University of Technology/ Baghdad.

Received on: 16/12/2013 & Accepted on: 5/3/2015

ABSTRACT

Aluminum doped nickel ferrite samples with composition $\text{NiFe}_{2-x}\text{Al}_x\text{O}_4$ (where; $x=0, 0.2, 0.4, 0.6, 0.8, 1, 1.2, 1.4$), were synthesized by using sol-gel auto combustion method at temperature about 200°C , then pelletized and sintered at different temperatures ($900, 1000, 1100$ and 1200°C). The present work focuses on studying the structural and electrical properties of Ni-Al ferrite by using many analysis's like x-ray diffraction, LCR meter, FTIR and AFM. The results show that the chemical composition has a major effect on electrical, structural, and physical properties. The result also showed that the dielectric constant and dielectric loss decreased with the increase of the Al content in Ni-Al ferrite sintered at 1200°C .

Keywords: Nanotechnology, spinel ferrites, sol-gel method,

دراسة الخصائص التركيبية والكهربائية لفرايتات النيكل المطعمة بأيونات الألمنيوم

الخلاصة:

حضرت نماذج فرايت النيكل المطعمة بأيونات الألمنيوم بطريقة الاحتراق الذاتي للمحلول الهلامي ذي التركيب عند درجة حرارة حوالي 200°C . (تاخذ القيم من الصفر الى القيمة $1.4 \times$ (حيث ان $\text{NiFe}_{2-x}\text{Al}_x\text{O}_4$ بعد ذلك تم جعلها بشكل اقراص ولبدت عند درجات حرارة مختلفة ($900, 1000, 1100, 1200$ درجة مئوية).

ركز البحث الحالي على دراسة الخصائص التركيبية والكهربائية لفرايت النيكل المطعم بالألمنيوم باستخدام النتائج بان التركيب الكيميائي الاثر الاكبر وظهرت LCR , AFM , XRD, FTIR تقنيات تحليلية عدة منها على الخصائص التركيبية والكهربائية والفيزيائية للفرايت المحضر. كما يتبين من النتائج بان ثابت العزل والفقد العزلي تتناقصان مع زيادة محتوى ايونات الألمنيوم في فرايت النيكل الملبد عند درجة الحرارة 1200°C .

الكلمات المفتاحية: التقنية النانوية، فرايتات السبيل، طريقة المحلول-الهلامي

INTRODUCTION

Nanotechnology is a broad interdisciplinary area of research, development and industrial activity which has been growing rapidly worldwide for the past decade. It can be defined as the branch of science and engineering where phenomena occur at the nanometer scale (1-100nm). Generally, nanotechnology deals with design, development, production and application of nonmaterials in devices and systems [1]. Nanoscience is the underpinning science of nanotechnology and it refers to study of phenomena and the manipulation of materials at the atomic, molecular and macromolecular scales, where properties differ significantly from those at a larger scale. Nanoscience is not just the science of small particles but the science in which the materials with small dimension show new physical phenomena, such as high surface to volume ratio, quantum confinement and discretization of energy. Due to these, the nonmaterial possess different properties giving rise to newer properties as compared to their at bulk counterparts [2].

Much research has been carried out on synthesis and characterization of iron oxide [3], cobalt ferrite [4], nickel ferrite [5], manganese ferrite [6], magnesium ferrite [7], and zinc ferrite nanoparticles [8]. The metal based ferrite nanoparticles have been synthesized by various methods as sol-gel auto combustion, evaporation condensation, template-based electrochemical synthesis, spray pyrolysis, micro-emulsion technique, reverse micelle, hydrothermal, and co-precipitation [5].

In the present investigation, we have employed sol-gel method to synthesize Al-doped nickel ferrite nanoparticles. This method offers a significant saving in time and energy consumption over the traditional methods, and requires less sintering temperature [9,10]. This method is employed to obtain improved powder characteristics, more homogeneity and narrow particle size distribution, thereby influencing structural and electrical properties of spinel ferrites. Therefore, this ferrite has numerous applications in recording heads, core materials for various transformers and inductors. In this work, $\text{NiFe}_{2-x}\text{Al}_x\text{O}_4$ fine powder was prepared by sol-gel method.

Materials and methods

Materials

The materials that had been used in the preparation process are Iron nitrate (12.12-36.36 gm), Nickel nitrate (14.53gm), Aluminum Nitrate (3.74-26.24 gm) and Citric acid (28.8 gm). The weight of nitrate material in the required ferrite structure was calculated by the molar weight. The following values ($x= 0, 0.2, 0.4, 0.6, 0.8, 1, 1.2, 1.4$) were used and after that mixed with (80ml) of distilled water. The mixture placed in a beaker and stirred by using magnetic stirrer at room temperature until get homogeneous solution.

Synthesis of $\text{NiFe}_{2-x}\text{Al}_x\text{O}_4$ ferrite nanoparticles

The preparation of homogeneous solution was done by continuous stirring with magnetic stirrer model (LMS-1003). The pH of the solution was adjusted to (~7). The ammonia solution was added in the form of drops till the PH reached 7 with continuous mixing by magnetic stirrer then the solution became brown color and then heated to 60°C for one hour. The temperature was then increased to 80°C with continuous stirring; the size of the solution became less. The gel began forming on the surface of the mixture, particularly in the middle and the solution was converted totally into a gel. The gel dried at 120°C for about three hours in an oven then the

temperature has been increased to 200° C. The dry gel began to change in shape and after short period, it was noted that a flame spreader in all directions to burn the top layer of dried gel and turned into a grid of columns converging dried gel burnt until all gels were completely burnt out to form a fluffy loose structure. The fluffy material was ground to get ferrite powder. The as-burnt ash was calcined at 500°C for 3hrs, to get better crystallization and homogeneous cation distribution in the spinel crystallite. Finally the powder was grounded to get ferrite powders. Later, we took out 1 gm of all composition calcined at 500°C for measurement of X-Ray diffraction. The powders mixed with 3 wt.% PVA (Polyvinyl alcohol) as a binder then a cold pressed by hydraulic press was applied into pellets of 10mm diameter under uniaxially load of 3tons. The samples were sintered at different temperatures of (900, 1000, 1100, 1200°C) for three hours.

Characterizations

The morphology, composition and structure of synthesized $\text{NiFe}_{2-x}\text{Al}_x\text{O}_4$ ferrite nanoparticles were studied by X-ray diffraction to measure phase Analysis and crystallite size by Debye Sheerer [11].

$$D = 0.9 \lambda / \beta \cos \theta \quad \dots(1)$$

Where

D is the crystallite size, λ is the wavelength of the radiation (1.54Å), θ is the Bragg's angle and β is the full width at half maximum (FWHM).

Lattice parameter (a) is the parameter defining the unit cell of a crystal lattice. Lattice constant refers to the constant distance between the lattice points. It can be determine from this equation:

$$a = \lambda (h^2 + k^2 + l^2)^{1/2} / 2 \sin \theta \quad \dots(2)$$

Where

(a) is lattice parameter, (λ) is the wavelength of the radiation, (θ) is the Bragg's angle and (hkl) is Miller index.

The X-ray density of the samples have been computed from the values of lattice parameters using the formula,[12]:

$$d_x = 8 M / N_a \cdot a^3 \quad \dots(3)$$

Where

(8) represents the number of molecules in a unit cell of spinal lattice, M the molecular weight of the sample, N_a the Avogadro's number and (a) represents the lattice constant of the sample.

LCR meter model (4294 A) is generally used for measurement of dielectric constant, dielectric loss and a.c. conductivity as a function of frequencies in the range (100 Hz- 5 MHz). Fourier Transform-Infrared Spectroscopy FTIR used to measures the molecular vibrations of molecules for the for ferrite samples. Atomic Force Microscope (AFM) analysis was done using scanning prop microscopy (CSPM). The AFM is an instrument capable of measuring the topography of a given sample. A nanosized tip attached on a cantilever was traced over the sample and a 3D image of the sample topography was generated on a computer. The advantage of the AFM over

SEM is the ability to make topographical measurements for detection and investigation of the size and shape of nanoparticles in three dimensions. Thus, the AFM makes it possible to determine the height of the particles.

Results and discussion

XRD analysis

X-ray diffraction patterns data of the $\text{NiAl}_x\text{Fe}_{2-x}\text{O}_4$ ferrite nanopowders calcined at temperatures (200, 500, 900, 1000°C) with $x=1.0$ is shown in Figures (1) to (6).

Diffraction pattern of the dried gel at 110°C does not show any peaks. XRD patterns of as-burnt ferrite powder at 200°C and calcined at 500°C for 3 h are shown in Figures (1) and (2). The broad peaks in the XRD patterns indicated fine crystallite size of the ferrite particles with compositions NiAlFeO_4 (for $x=1$). This behavior indicated that the Ni-Al ferrite can be directly formed after the auto combustion of the gel without calcinations. The crystallite size of the as-burnt powder was estimated from the X-ray peak broadening of the (311) diffraction peak using Scherrer formula (see equation 1). This showed that the synthesized powder has nano-sized crystallite. As expectation the crystallite size increased with successive heat treatment of the ferrite powders.

Strongest diffraction peaks (311) and (400) were found in figure (1), while the planes (311), (400) and (220) were found in figure (2). The peak intensity for all planes depended upon the concentration of magnetic ions in the lattice. The decrease in x-rays broadening decreased with the increase in calcination temperature was attributed to the grain growth of crystallites at higher temperatures.

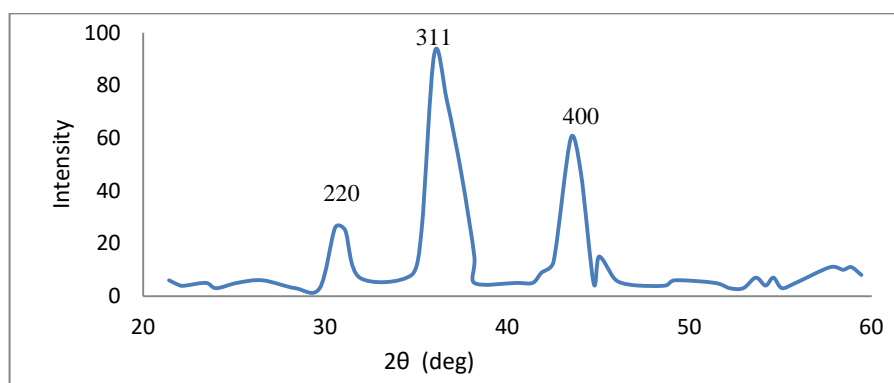


Figure (1): XRD patterns of as burnt powder ($\text{NiFe}_{2-x}\text{Al}_x\text{O}_4$) at 200° C

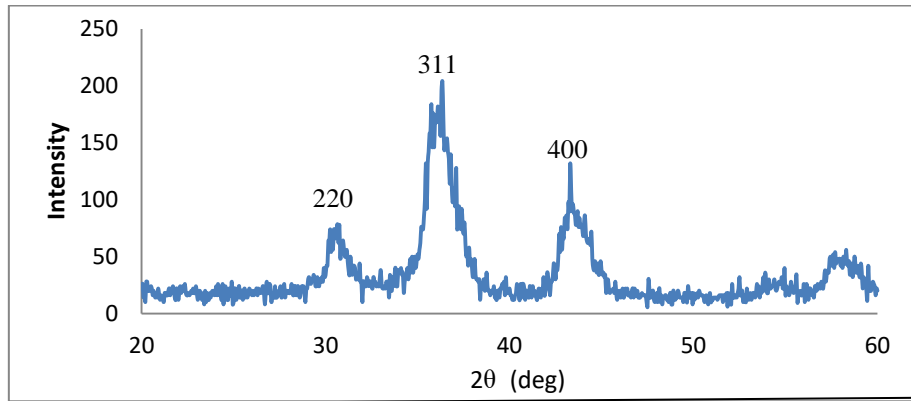


Figure (2): XRD patterns of $(\text{NiFe}_{2-x}\text{Al}_x\text{O}_4)$ powder calcined at 500°C

Strongest diffraction peaks (311), (220) and (511) were found in the diffraction pattern which confirmed the formation of pure phase spinel structure in all samples sintered at 900 , 1000 , 1100 , 1200°C in figures (3),(4),(5) and (6) respectively. The broadening in X-rays spectrum was decreased with the increase in sintering temperatures which attributed to the grain growth of the crystallites at higher temperatures.

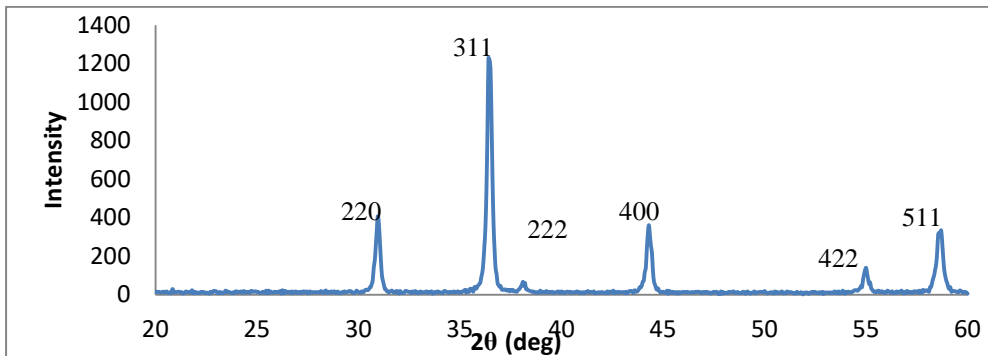


Figure (3): XRD patterns of $(\text{NiFe}_{2-x}\text{Al}_x\text{O}_4)$ samples sintered at 900°C

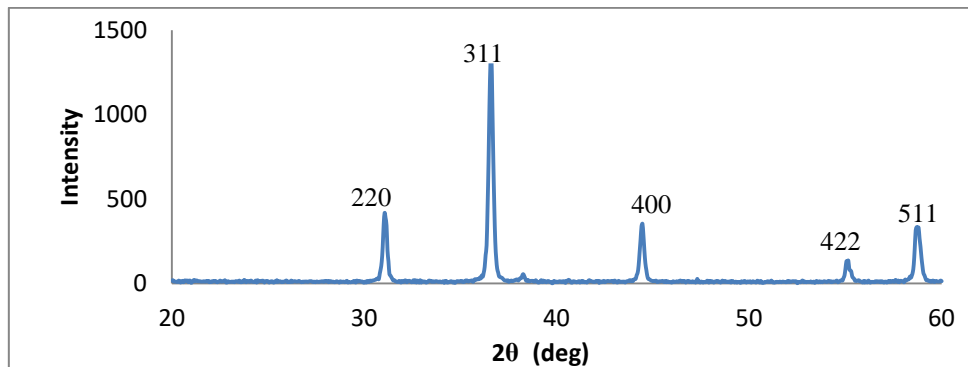


Figure (4): XRD patterns of $(\text{NiFe}_{2-x}\text{Al}_x\text{O}_4)$ samples sintered at 1000°C

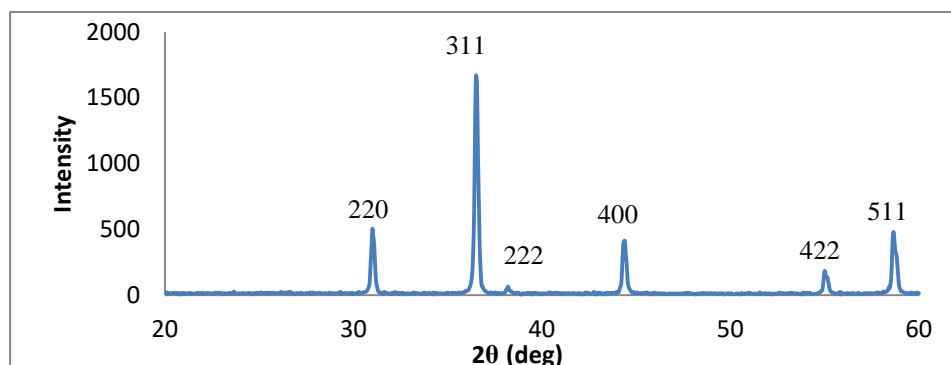


Figure (5): XRD patterns of $\text{NiFe}_{2-x}\text{Al}_x\text{O}_4$ samples sintered at 1100°C

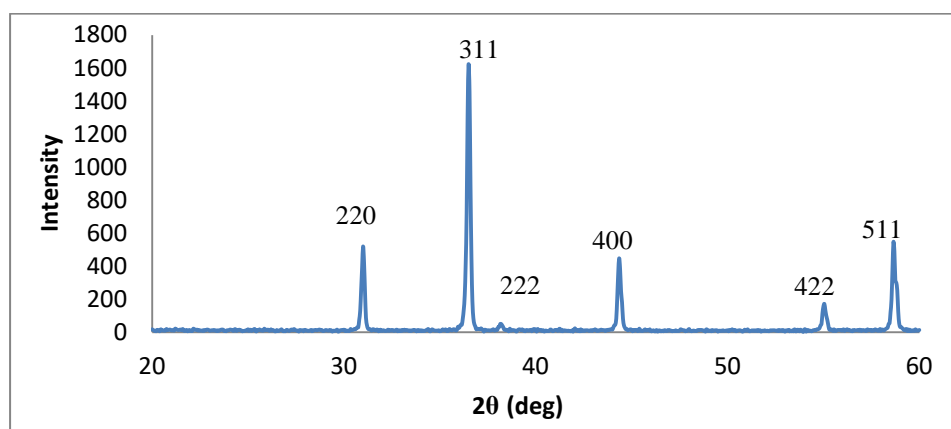


Figure (6): XRD patterns of $\text{NiFe}_{2-x}\text{Al}_x\text{O}_4$ samples sintered at 1200°C

Lattice constant, crystallite size and X-ray density of $\text{NiFe}_{2-x}\text{Al}_x\text{O}_4$ samples

Lattice constant, crystallite size and X-ray density of NiFeAlO_4 nanoferrite were calculated by using equations (1),(2) and (3) listed in table (1), it was found that the lattice constant decreased with increasing calcination or sintering temperatures. While, the lattice constant and X-ray density of the NiFeAlO_4 samples increases with increasing calcination and sintering temperatures as shown in table (1).

Table (1): Lattice constant, Crystallite size, x-ray density of $\text{NiFe}_{2-x}\text{Al}_x\text{O}_4$ ferrite samples

| Sintering Temp. $^\circ\text{C}$ | Latticeconstant (a) Å^0 | Crystallite size (nm) | X-ray density g/cm^3 |
|--|----------------------------------|-----------------------|-------------------------------|
| As burnt Powder at 200°C | 8.2703 | 5.64537 | 4.8266 |
| Calcined at 500°C | 8.217 | 7.0306 | 4.9210 |
| 900°C | 8.1669 | 10.346 | 5.0121 |
| 1000°C | 8.1401 | 11.76 | 5.0363 |
| 1100°C | 8.15140 | 14.4615 | 5.0408 |
| 1200°C | 8.1538 | 20.470 | 5.0618 |

FTIR analysis

The FTIR bands of solids are usually assigned to vibration of ions in the crystal lattice [13]. The FTIR spectra of nano crystalline $\text{NiFe}_{2-x}\text{Al}_x\text{O}_4$ ferrite samples were charted in the range of 300 cm^{-1} to 4000 cm^{-1} as shown in Figure (7). The spectra of the dried gel at (110°C), as-burnt powder at (200°C) and calcined powder at 500°C of NiFeAlO_4 ferrite samples were illustrated in figure (7). When the heat treatment increased the degree of crystallization was increased as shown in figures (7a) and (7b). The higher frequency band (ν_1) ($545\text{--}585\text{ cm}^{-1}$) and lower frequency band (ν_2) ($365\text{--}395\text{ cm}^{-1}$) are assigned to the tetrahedral and octahedral complexes. It explains that the normal mode of vibration of tetrahedral cluster is higher than that of octahedral cluster. It should be attributed to the shorter bond length of tetrahedral cluster and longer bond length of octahedral cluster.

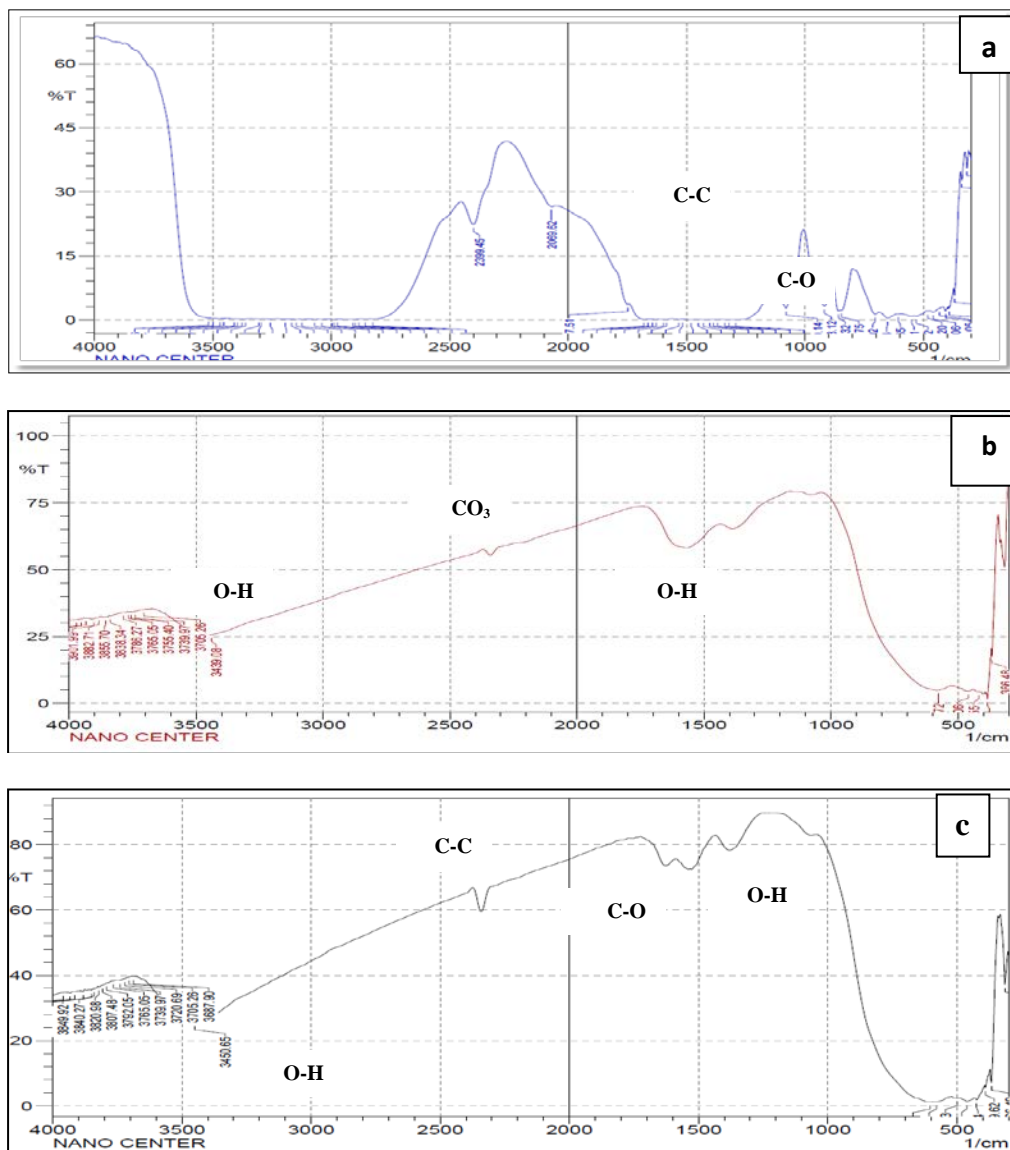


Figure (7) : FTIR spectra of; (a) dry gel at 110°C , (b) as-burnt powder at 200°C , (c) Calcined powder at 500°C of $(\text{NiFe}_{2-x}\text{Al}_x\text{O}_4)$ nanoferrite

Atomic Force Microscope (AFM)

The atomic force microscope is one of the types of scanning probe microscopes, which is used to image surface structures on a nm or even sub-nm level and to measure surface forces. AFM used for topographical imaging, was used to look at the structure of NiFeAlO₄ as the top layer.

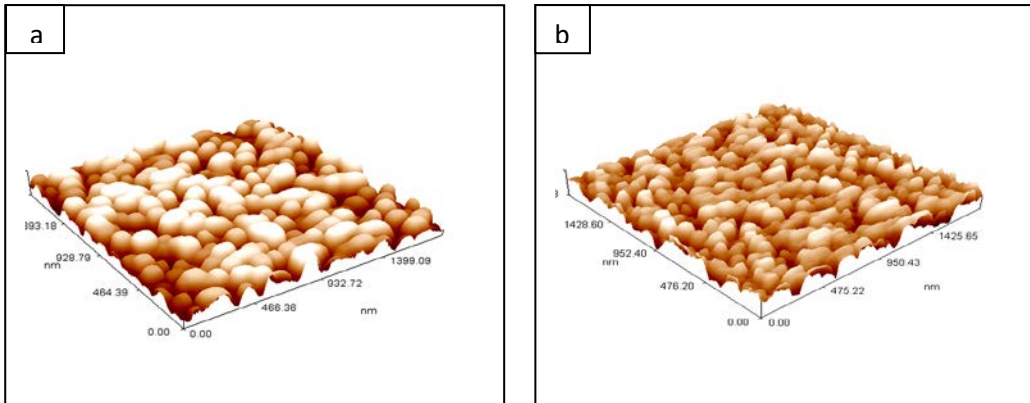


Figure (8): Surface morphology 3D image (a) AFM for as-burnt powder at 200 °C (b) AFM for calcined sample at 500 °C for NiFe_{2-x}Al_xO₄ ferrite nanopowders

The mean grain size and roughness were increased with sintering temperature. The mean crystallite size ($\approx 11\text{nm}$) obtained by using Scherrer-Debye formula were smaller than that observed ($\approx 60\text{nm}$) in AFM images indicating these particles probably an aggregate of many crystallite or may be due to AFM was the surfacemorphology of coalesced grains which gave the particle size.

Any variation in the dielectric constant with the change in composition depends upon the difference in the ionic radii of the constituent elements. It was observed that dielectric constant increased with the increasing Al-ion content (x) in NiAl_xFe_{2-x}O₄ ferrites as shown in figure (9) sintered at 1200°C.

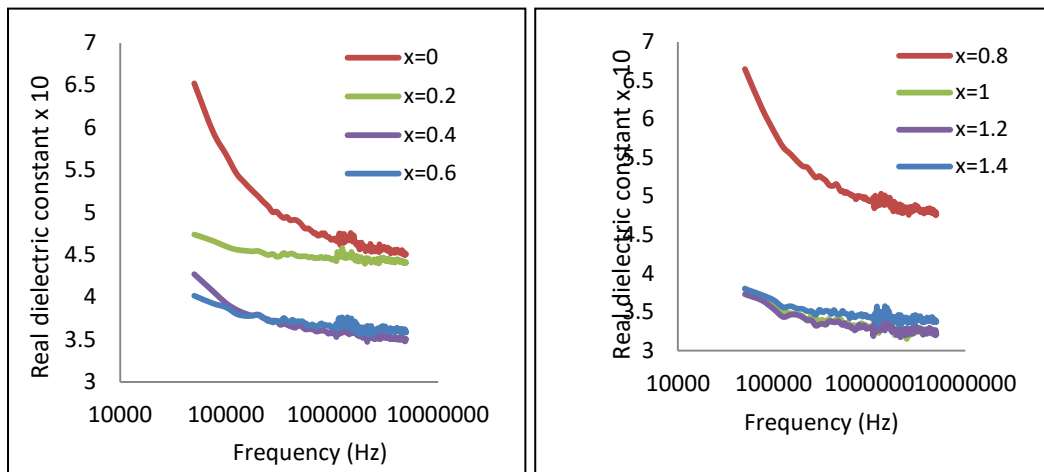


Figure (9): Variation of the real dielectric constant with frequency of NiAl_xFe_{2-x}O₄ With (x=0.0 - 1.4) sintered at temp. 1200°C

In Ni-Al ferrites, Al-ions occupy tetrahedral (A) sites whereas nickel ions prefer to go to octahedral (B) sites. Consequently, polarization and dielectric constant increase, but found the value of (ϵ_r') decreases at $x=1.4$. Variation of dielectric constant (ϵ_r') with frequency is shown in figures (9), it is clear from the figure dielectric constant decrease with increasing frequency. This decrease in dielectric constant with frequency is normal dielectric behavior of spinel ferrites, it can be explained by Maxwell-Wagner two layers model of interfacial polarization with Koop's phenomenological, which supposed that the ferrite compact acts as multilayer capacitor.

The data on the dielectric loss factor ($\tan \delta$), is used to study the Al-ion addition on the loss characteristics of the $\text{NiAl}_x\text{Fe}_{2-x}\text{O}_4$ ferrite. Figure (10) shows the loss behavior of the sample sintered at 1200°C with ($x=0, 0.2, 0.4, 0.6, 0.8, 1, 1.2, 1.4$), and it is clear that the dielectric loss tangent are found to decrease with the applied frequency increase. This decrease in ($\tan \delta$) with frequency occurs because of the fact that hopping frequency of the charge carrier doesn't follow the change of polarity of the external a.c. field beyond a certain frequency. The initial decrease in $\tan \delta$ with an increase in frequency may also be explained on the basis of Koop's phenomenological.

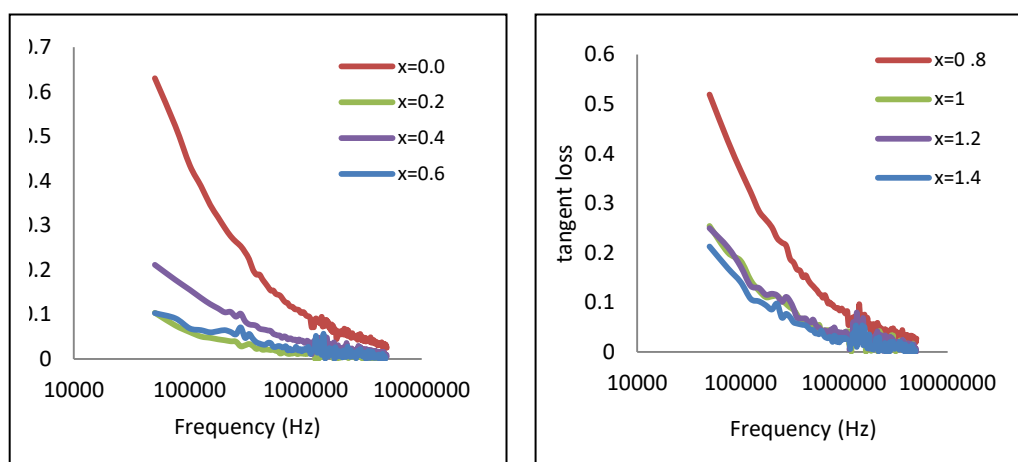


Figure (10): Variation of the loss tangent with frequency of $\text{NiAl}_x\text{Fe}_{2-x}\text{O}_4$ with ($x=0.0 - 1.4$) sintered at temp. 1200°C

Conclusions

NiAlFeO_4 ferrites were prepared by the sol-gel autocombustion method. The X-ray density and crystallite size of all the samples increases with increase in calcination or sintering temperatures. While the lattice constant (a) decreases with calcination or sintering temperatures. The crystallite sized of ferrite powder which are resulted in Auto combustion process in Nano range about of (5-20 nm) with crystalline spinel ferrite structure.

The prepared $\text{NiAl}_x\text{Fe}_{2-x}\text{O}_4$ samples with ($0 \leq x \leq 1.4$) sintered at 1200°C for three hours are found that the dielectric constant and loss tangent decreases with increasing frequency for all the samples.

References

- [1] M. W. Barsoum; "Fundamentals of Ceramics". McGraw-Hill company, Inc., New York, (1997).
- [2] Philip Moriarty, Rep. Prog. Phys. 64 297–381, (2001)
- [3] Carlos S. Kuroda^I, Takuma Shimura^P, Masahito Maeda^P, Masaru Tada^P, Hiroshi Handa^Q, Adarsh Sandhu^R, and Masanori Abe, IEEE Transactions on Magnetic, Vol. 42, No. 10, October (2006).
- [4] Jae-Gwang Lee, Hi Min Lee, Chul Sung Kim, Young Jei-Oh, Journal of Magnetism 177-181 900-902, (1998)
- [5] K. Maaz, S. Karim, A. Mumtaz, S.K. Hasanain, J. Liu, J.L. Duan, Journal of Magnetism and Magnetic Materials 321 1838-1842, (2009)
- [6] Irfan Elahi, Rabab Zahira, Kiran Mehmood, Arifa Jamil and Nasir Amin, African Journal of Pure and Applied Chemistry Vol. 6(1), pp. 1-5, 10 January, (2012).
- [7] A. Pradeep, P. Priyadharsini, G. Chandrasekaran, Journal of Magnetism and Magnetic Materials 320 2774-2779, (2008)
- [8] A. Gatelyte, D. Jasaitis, A. Beganskiene, A. Kareiva, ISSN 1392–1320 Materials Science, Vol. 17, No. 3, (2011)
- [9] Raghavender A.T., Pajic D., Zadro K., Milekovic T., Venkateshwar Rao P., Jadhav K.M. and Ravinder D., "Synthesis and magnetic properties of NiFe_{2-x}Al_xO₄ nanoparticles", J. Magn. Mater., 316, 1-7 (2007).
- [10] Raghavender A.T., Kulkarni R. G. and Jadhav K.M., "Magnetic Properties of Nanocrystalline Al Doped Nickel Ferrite Synthesized by the Sol-Gel Method", Chinese Journal of Physics, 46, 366-375, (2007) .
- [11] D. Garmos, "Materials and Processes in Manufacturing" ; Wiley, 10th Edition, (2007).
- [12] McColm, I. J. & Clark, N. J. Forming, Shaping and Working of High-Performance Ceramics. Blackie, Glasgow, pp. 1-338, (1988).
- [13] N. A. D. Burke, H. D. H. Stover, F. P. Dawson, Chem. Mater 14, 4752-4761, (2002).